Mondati, G., Giaccio, B., Deino, A.L., Arcangeli, P., Bertini, A., Huang, H., Nocentini, M., Iorio, M., Angelino, A., Cifelli, F., Mattei, M., Sagnotti, L., Gliozzi, E., Marchegiano, M., Petrelli, M., Peral, M., Claeys, P., Regattieri, E., Zanchetta, G., Spadi, M., Tallini, M., Conte, A.M., Conticelli, S., Casalini, M., Racano, S., and Cosentino D., 2025, Constraining the early stage of the post-orogenic extensional tectonics in central Italy: New evidence from a long sediment core from the tectonically active L'Aquila Basin: GSA Bulletin, https://doi.org/10.1130/B37760.1.

Supplemental Material

Table S1. Multi-crystal total fusion (MCTF) analyses of a feldspar population from SNC-2 tephra.

Table S2. Multi-crystal incremental heating (MCIH) analyses of a feldspar population from SNC-2 tephra.

Table S3. Clumped carbonate isotope (Δ_{47}) analyses and relative temperature values (T).

Table S4. WDS major element composition of the glass from tephra SNC-2 and CN-29.38.

Figure S1. CN-1 sediment core between -115 m to -120 m**.**

Figure S2. CN-1 sediment core between -120 m to -125 m.

Figure S3. CN-1 sediment core between -125 m to -130 m.

Figure S4. CN-1 sediment core between -70.24 m to -70.40 m, showing the presence of a single outsized carbonate clast ("dropstone").

Figure S5. CN-1 sediment core between -126.00 m to -126.19 m, showing the presence of a single outsized carbonate clast ("dropstone").

Figure S6. CN-1 sediment core between -137.51 m to -137.69 m, showing the presence of a single outsized carbonate clast ("dropstone").

Figure S7. CN-1 sediment core between -25.00 m to -30.00 m. The black layer between -29.28 m to -29.38 m is the tephra (CN 29.38) that corresponds to the tephra sampled from a cellar of Castelnuovo village (SNC-2), which has been 40Ar/39Ar dated to 1.77 ± 0.15 Ma.

Figure S8. CN-1 sediment core between -180.00 m to -185.00 m.

Figure S9. CN-1 sediment core between -195.00 m to -200.00 m.

Figure S10. CN-1 sediment core between -220.00 m to -223.00 m.

Figure S11. Representative demagnetization plots for selected specimens subjected to stepwise thermal demagnetization (a, b, c) and to stepwise AF demagnetization (d, e, f). The samples show demagnetization vectors aligned along linear paths towards the origin, after removal of a viscous low coercivity remanence component at the first demagnetization steps (5–10 mT for AF demagnetization; below 180-230°C for thermal demagnetization). For all the measured specimens a Characteristic Remanent Magnetization (ChRM) was determined by principal component analysis. The maximum

angular deviation (MAD) for each determined ChRM direction was 4° on average, with a full range of variation between 0.5° and 21° for the specimens treated by AF demagnetization, and it was 6° on average, with a full range of variation between 0.6° and 31°, for the specimens treated by thermal demagnetization. Diagrams in a) and d) show typical behaviour for specimens with clear reverse polarity; specimens b) and e) show typical behaviour for specimens with clear normal polarity; diagrams in c) show typical behaviour for specimens with a maximum unblocking temperature (Tub) of 360 °C; diagrams in f) show typical behaviour for specimens which acquire a significant gyroremanent magnetization (GRM) at AF steps higher than 40-50 mT. The GRM acquisition is perpendicular to the axis of the magnetometer (i.e., perpendicular to the Z-axis of the specimens) and to the direction of the last AF demagnetization. Orthogonal vector diagrams: open and closed symbols represent projections onto vertical and horizontal planes, respectively.

Figure S12. Periodogram showing main spectral density peaks highlighted by Multi-taper Method (MTM) spectral analysis, AR(1) modelling applied. Main frequency of 0.034814 cycles/m is related to a wavelength of 28.7240 m, with a secondary main peak marked by a frequency of 0.043976 cycles/m, referring to a wavelength of 22.7396 m.

Figure S13. Splitting of the raw calcimetry data series. (A) First isolated sector of the calcimetry signal. (B) Periodogram of the first isolated sector of the calcimetry signal with the AR(1) modelling option. (C) Second isolated sector of the calcimetry signal. (D) Periodogram of the second isolated sector of the calcimetry signal with the AR(1) modelling option.

Figure S14. Filter output from the raw calcimetry data series after applying a Gaussian band-pass filter for filtering the main frequency. (A) 12 m filter output of the first isolated sector of the calcimetry signal. (B) 25 m filter output of the second isolated sector of the calcimetry signal. (C) Merged output filter of the whole calcimetry time series.

TABLES

Table S1 – *Multi-crystal total fusion (MCTF) analyses of a feldspar population from SNC-2 tephra*

Lab ID#	J		Relative Isotopic Abundances										Derived Results						Inverse Isochron Data				
			^{40}Ar		^{39}Ar		^{38}Ar		^{37}Ar		^{36}Ar		^{39}Ar Mol	Ca/K		$^{40}Ar^{*}/^{39}Ar$		$\%^{40}Ar^{*}$	Age (Ma)	$^{36}Ar/^{40}Ar$		$^{39}Ar/^{40}Ar$		$^{38}Ar/^{39}Ar$
	(X 10^{-3})	±1σ		±1σ		±1σ		±1σ		±1σ		±1σ	∞ 10^{-18}		±1σ		±1σ		±1σ		±%1σ		±%1σ		Er. Corr.
27573-02A	0,122	0,000	2850	150	164,4	1,8	3,1	1,1	656	6	5,5	1,0	5,64	11,67	0,16	7,7950	± 2,1009	44,8	1,70	0,47	0,00185	20,40	0,05748	5,32	0,2492
27573-02A	0,122	0,000	2890	150	213,3	2,0	3,1	1,1	1197	6	4,8	1,0	7,21	16,43	0,17	7,5985	± 1,6338	55,7	1,70	0,37	0,00148	25,00	0,07330	5,14	0,1987
27573-07A	0,122	0,000	9600	70	246,2	1,8	7,4	1,2	943	5	24,9	0,9	8,42	16,43	0,15	9,4979	± 1,1274	24,2	2,10	0,25	0,00254	3,74	0,02551	1,02	0,1311
27573-08A	0,122	0,000	4110	70	277,1	1,9	5,4	1,1	1318	6	7,6	0,8	9,48	20,43	0,16	7,4495	± 0,8662	49,9	1,67	0,19	0,00168	11,20	0,06696	1,78	0,1350

Table S2 – *Multi-crystal incremental heating (MCIH) analyses of a feldspar population from SNC-2 tephra*

Lab ID#	Watts	J		Relative Isotopic Abundances										Derived Results								Inverse Isochron Data				
				^{40}Ar		^{39}Ar		^{38}Ar		^{37}Ar		^{36}Ar		^{39}Ar Mol	^{39}Ar %	$\%(^{36}Ar)_{Ca}$	Ca/K		$^{40}Ar^{*}/^{39}Ar$		$\%\ ^{40}Ar^{*}$	Age (Ma)	$^{36}Ar/^{40}Ar$		$^{39}Ar/^{40}Ar$		$^{38}Ar/^{39}Ar$
		(X 10^{-3})	±1σ		±1σ		±1σ		±1σ		±1σ			∞ 10^{-18}	of total			±1σ		±1σ		±1σ	±%1σ		±%1σ		Er. Corr.
27573-01A	0,9	0,1224	0,0002	70	170	0,5	1,5	3,2	1,3	-1	5	-0,8	1,0	**0,0**	0,1	0,0		30	551,55	1645,17	407,1	100,00	300,00	- 0,01029	-276,58	0,00738	361,28	0,5643
27573-01B	1,3	0,1224	0,0002	440	170	3,5	1,5	-0,2	1,0	8	5	2,3	1,1	**0,1**	0,5	0,1	6	5	-73,04	107,99	-56,7	-20,00	20,00	0,00531	60,74	0,00885	57,79	0,4460
27573-01C	1,8	0,1224	0,0002	1380	170	40,4	1,6	0,0	1,4	291	5	3,6	1,1	**2,1**	11,7	3,0	13,6	0,4	5,31	6,21	23,2	1,20	1,40	0,00257	33,67	0,04368	7,95	0,3675
27573-01D	2,5	0,1224	0,0002	2320	170	177,5	1,9	4,6	1,3	781	6	4,2	1,1	**6,9**	34,3	7,1	12,46	0,16	6,59	2,13	50,2	1,50	0,50	0,00167	29,80	0,07610	7,46	0,2442
27573-01E	3,4	0,1224	0,0002	1420	170	109,2	1,7	0,4	1,1	546	6	2,8	1,1	**3,7**	21,1	7,5	14,2	0,3	6,18	3,12	46,8	1,40	0,70	0,00178	43,37	0,07573	12,00	0,2718
27573-01F	4,6	0,1224	0,0002	840	170	80,5	1,6	0,1	1,1	412	5	0,2	1,1	**2,7**	15,6	101,2	14,5	0,4	10,51	4,60	100,1	2,40	1,00	0,00000	-58307,23	0,09518	20,38	0,0003
27573-01G	6,4	0,1224	0,0002	700	170	75,0	1,6	2,0	1,3	367	5	1,4	1,1	**2,5**	14,1	10,2	14,3	0,4	4,58	4,97	47,5	1,00	1,10	0,00176	89,76	0,10366	24,44	0,2701
27573-01H	9,0	0,1224	0,0002	310	170	12,9	1,5	-0,6	1,2	64	5	0,6	1,1	**0,4**	2,5	4,2	14	2	11,01	28,31	46,1	2,00	6,00	0,00181	201,87	0,04188	56,83	0,2690
27573-04A	1,0	0,1224	0,0002	960	60	40,2	1,4	0,3	1,1	124	5	2,6	0,7	**1,4**	9,0	2,8	13,1	0,7	5,42	5,40	22,5	1,20	1,20	0,00260	28,42	0,04151	7,28	0,1937
27573-04B	1,7	0,1224	0,0002	5330	60	168,2	1,7	5,5	1,2	560	5	12,6	0,8	**5,5**	35,9	2,6	14,9	0,2	10,52	1,51	31,4	2,40	0,30	0,00230	6,46	0,02988	1,56	0,1325
27573-04C	2,9	0,1224	0,0002	1190	60	95,2	1,4	-0,9	1,2	351	5	1,0	0,7	**3,2**	20,9	21,2	16,1	0,3	10,40	2,25	81,2	2,30	0,50	0,00063	89,20	0,07801	5,39	0,0554
27573-04D	4,9	0,1224	0,0002	400	60	37,9	1,3	-3,8	1,3	136	5	0,2	0,7	**1,3**	8,5	38,5	15,4	0,8	9,27	5,65	86,8	2,10	1,30	0,00044	382,42	0,09556	15,44	0,0364
27573-04E	8,4	0,1224	0,0002	659	60	86,1	1,4	-2,5	1,3	304	5	0,2	0,7	**2,9**	19,3	98,2	15,1	0,4	7,60	2,57	99,8	1,70	0,60	0,00001	20704,06	0,13137	9,60	0,0004
27573-04F	14,2	0,1224	0,0002	270	60	29,0	1,2	-0,6	1,2	108	5	0,1	0,7	**1,0**	6,5	57,0	15,8	1,0	8,88	7,71	94,8	2,00	1,70	0,00017	1510,72	0,10681	23,45	0,0149
27573-05A	1,0	0,1224	0,0002	1080	60	29,5	1,3	-1,2	1,1	36	5	2,8	0,8	**1,0**	7,5	0,7	5,2	0,7	7,94	8,69	21,7	1,80	1,90	0,00262	29,87	0,02728	7,42	0,1573
27573-05B	1,7	0,1224	0,0002	1680	60	142,2	1,6	2,0	1,1	361	5	2,8	0,7	**4,9**	36,1	7,5	10,84	0,20	6,51	1,58	54,7	1,40	0,40	0,00152	28,10	0,04406	3,98	0,1288
27573-05C	2,9	0,1224	0,0002	1700	60	151,4	1,5	5,0	1,2	432	5	1,3	0,7	**5,2**	38,4	18,4	12,18	0,19	9,07	1,42	80,7	2,00	0,30	0,00065	62,35	0,08891	3,99	0,0601
27573-05D	4,9	0,1224	0,0002	510	60	65,3	1,3	1,9	1,2	183	5	-0,4	0,7	**2,2**	16,1	-28,8	12,4	0,4	10,34	3,47	127,3	2,30	0,80	- 0,00092	-148,97	0,12334	12,86	0,0841
27573-05E	8,4	0,1224	0,0002	10	60	7,4	1,2	-0,4	1,2	29	5	-0,9	0,7	**0,3**	1,9	- 1,8	17	4	39,71	31,45	3937,1	9,00	7,00	- 0,12655	-878,08	0,99165	874,92	0,9961
27573-06A	1,0	0,1224	0,0002	950	60	22,0	1,2	0,7	1,0	40	5	2,4	0,7	**0,8**	6,3	0,9	7,8	1,0	10,53	10,31	24,2	2,00	2,00	0,00254	30,71	0,02301	8,69	0,1735
27573-06B	1,7	0,1224	0,0002	3190	60	250,4	1,8	1,6	1,2	791	5	4,3	0,7	**8,6**	71,1	10,6	13,52	0,13	8,22	0,89	64,2	1,80	0,20	0,00120	18,74	0,07815	2,18	0,1018
27573-06C	2,9	0,1224	0,0002	420	60	53,8	1,4	-0,3	1,0	184	5	0,4	0,7	**1,8**	15,3	26,3	14,6	0,5	6,12	4,03	78,7	1,40	0,90	0,00071	232,26	0,12864	15,96	0,0670
27573-06D	4,9	0,1224	0,0002	240	70	25,8	1,3	1,1	1,0	94	5	0,3	0,7	**0,9**	7,3	16,8	15,6	1,1	6,34	9,02	67,0	1,00	2,00	0,00110	279,46	0,10575	27,70	0,0962

Table S3 - *Clumped carbonate isotope (Δ_{47}) and relative standard error (SE); temperature values (T) using Anderson et al. (2021) equation and relative two-times standard error (2SE).*

Sample	***Depth (m)***	***N° replicates***	***Δ_{47} (‰)***	***SE***	***Δ_{47}-T (°C)***	***2SE***
ETH-4		*94*	*0.4496*	*0.0044*		
CN15-4	*14.04*	*10*	*0.6367*	*0.0084*	*11.5*	*1.3*
CN20-69	*19.69*	*8*	*0.6235*	*0.0091*	*15.4*	*1.6*
CN29-14	*28.14*	*6*	*0.6374*	*0.0101*	*11.3*	*1.8*
CN85-4	*86.04*	*7*	*0.6231*	*0.0097*	*15.6*	*1.7*
CN107-84	*108.84*	*7*	*0.6058*	*0.0094*	*21*	*1.7*

Table S4 - *WDS major element composition of the glass from tephra SNC2 and CN-29.38*

CN-29.38																						
SiO_2	57.7	61.6	60.9	60.5	63.4	58.5	58.9	56.9	56.4	59.3	59.6	60.3	59.2	58.8	58.6	58.4	56.4	57.4	59.8	57.5	58.2	57.0
TiO_2	0.90	1.01	0.90	0.77	0.71	1.34	1.02	0.79	0.98	0.78	0.81	0.91	0.91	0.99	0.95	0.88	1.05	0.94	0.79	0.78	1.00	0.73
Al_2O_3	16.7	15.6	16.5	17.7	17.5	15.7	15.6	18.3	16.7	17.2	17.1	16.8	15.9	16.5	16.4	16.6	16.1	16.9	16.5	16.6	17.0	17.9
FeO	7.55	6.92	6.01	6.05	4.04	9.76	8.10	7.37	7.01	7.08	5.99	6.80	7.21	7.67	7.86	6.78	8.52	8.36	7.20	8.74	6.81	7.58
MnO	0.24	0.18	0.17	0.16	0.16	0.24	0.23	0.21	0.22	0.23	0.20	0.21	0.19	0.24	0.18	0.12	0.15	0.12	0.15	0.19	0.11	0.28
MgO	3.05	2.30	1.75	1.43	1.25	1.86	2.43	2.85	2.56	2.47	2.46	1.50	2.68	2.64	2.65	2.34	4.11	2.82	2.59	3.33	2.11	3.10
CaO	7.64	6.50	6.61	6.18	4.13	5.49	6.98	7.16	10.1	5.97	7.09	6.19	6.93	6.98	6.84	7.94	8.08	7.13	6.26	6.01	8.07	7.67
Na_2O	3.13	2.22	3.31	3.16	3.40	3.41	3.01	3.14	2.90	3.22	3.24	3.36	3.04	3.04	3.12	3.14	3.03	3.17	3.22	3.36	3.38	3.20
K_2O	3.02	3.31	3.67	3.93	5.03	3.44	3.51	3.11	2.97	3.57	3.26	3.79	3.69	2.90	3.16	3.70	2.41	2.93	3.38	3.24	3.24	2.37
P_2O_5	0.13	0.33	0.21	0.14	0.33	0.18	0.22	0.17	0.18	0.20	0.23	0.14	0.27	0.21	0.21	0.15	0.11	0.20	0.18	0.18	0.13	0.16
F	0.00	0.13	0.15	0.10	0.25	0.05	0.13	0.17	0.16	0.26	0.00	0.08	0.08	0.20	0.11	0.10	0.00	0.34	0.15	0.01	0.17	0.12
Cl	0.21	0.22	0.27	0.26	0.19	0.16	0.23	0.21	0.24	0.27	0.14	0.29	0.24	0.23	0.23	0.21	0.13	0.19	0.24	0.22	0.21	0.16
SO_3	0.02	0.32	0.03	0.00	0.00	0.04	0.00	0.03	0.02	0.03	0.15	0.09	0.14	0.03	0.00	0.06	0.00	0.04	0.02	0.02	0.02	0.06
Alkali sum	6.15	5.54	6.98	7.10	8.42	6.86	6.52	6.25	5.87	6.78	6.51	7.15	6.73	5.94	6.28	6.84	5.44	6.10	6.60	6.61	6.62	5.57
Anlytical total	98.80	95.35	97.36	97.49	97.39	99.11	98.59	98.99	98.91	98.82	98.03	97.76	96.67	98.52	98.71	98.70	99.06	98.82	98.23	97.98	98.44	99.22

SNC-2																
SiO_2	59.1	58.4	58.6	65.0	59.9	57.9	60.48	59.1	57.2	58.6	63.4	57.5	60.40	61.3	62.4	60.1
TiO_2	1.05	1.06	1.09	0.76	0.93	0.84	0.98	0.79	0.78	1.07	0.65	1.11	1.28	1.03	1.34	0.98
Al_2O_3	17.1	16.1	15.6	15.8	16.3	17.0	14.9	19.0	16.6	16.2	15.4	15.9	14.9	17.7	15.4	19.0
FeO	7.30	7.97	8.67	4.77	6.93	7.89	7.56	5.45	9.07	8.26	5.55	8.94	8.72	5.38	6.79	4.74
MnO	0.20	0.12	0.14	0.10	0.17	0.18	0.21	0.09	0.13	0.14	0.11	0.20	0.13	0.08	0.18	0.20
MgO	1.82	3.14	3.31	1.18	3.46	2.79	2.53	1.41	3.49	2.22	2.07	3.00	2.18	1.17	1.38	0.96
CaO	7.39	7.55	6.62	3.80	6.14	7.06	6.98	8.01	6.49	6.92	5.19	6.93	5.38	5.73	4.45	6.66
Na_2O	3.13	2.74	2.78	4.46	3.30	3.22	2.89	3.13	3.14	3.21	3.14	2.63	3.00	3.57	3.03	3.60
K_2O	2.68	2.70	3.02	3.88	2.75	3.04	3.34	2.82	2.92	3.25	4.42	3.59	3.87	3.86	4.70	3.56
P_2O_5	0.22	0.16	0.17	0.23	0.16	0.18	0.15	0.19	0.17	0.16	0.08	0.23	0.19	0.24	0.33	0.16
F	0.00	0.13	0.07	0.00	0.03	0.22	0.30	0.12	0.02	0.16	0.05	0.03	0.11	0.03	0.25	0.08
Cl	0.05	0.14	0.16	0.21	0.10	0.23	0.25	0.24	0.20	0.25	0.26	0.15	0.18	0.12	0.13	0.09
SO_3	0.00	0.01	0.05	0.00	0.02	0.00	0.03	0.02	0.02	0.00	0.08	0.01	0.02	0.00	0.01	0.00
Alkali sum	5.81	5.44	5.80	8.35	6.06	6.25	6.23	5.94	6.06	6.46	7.56	6.22	6.87	7.43	7.73	7.16
Anlytical total	98.68	101.08	100.93	101.09	101.07	99.67	99.33	96.84	99.91	99.49	95.89	98.76	97.50	97.61	97.47	98.64

FIGURES

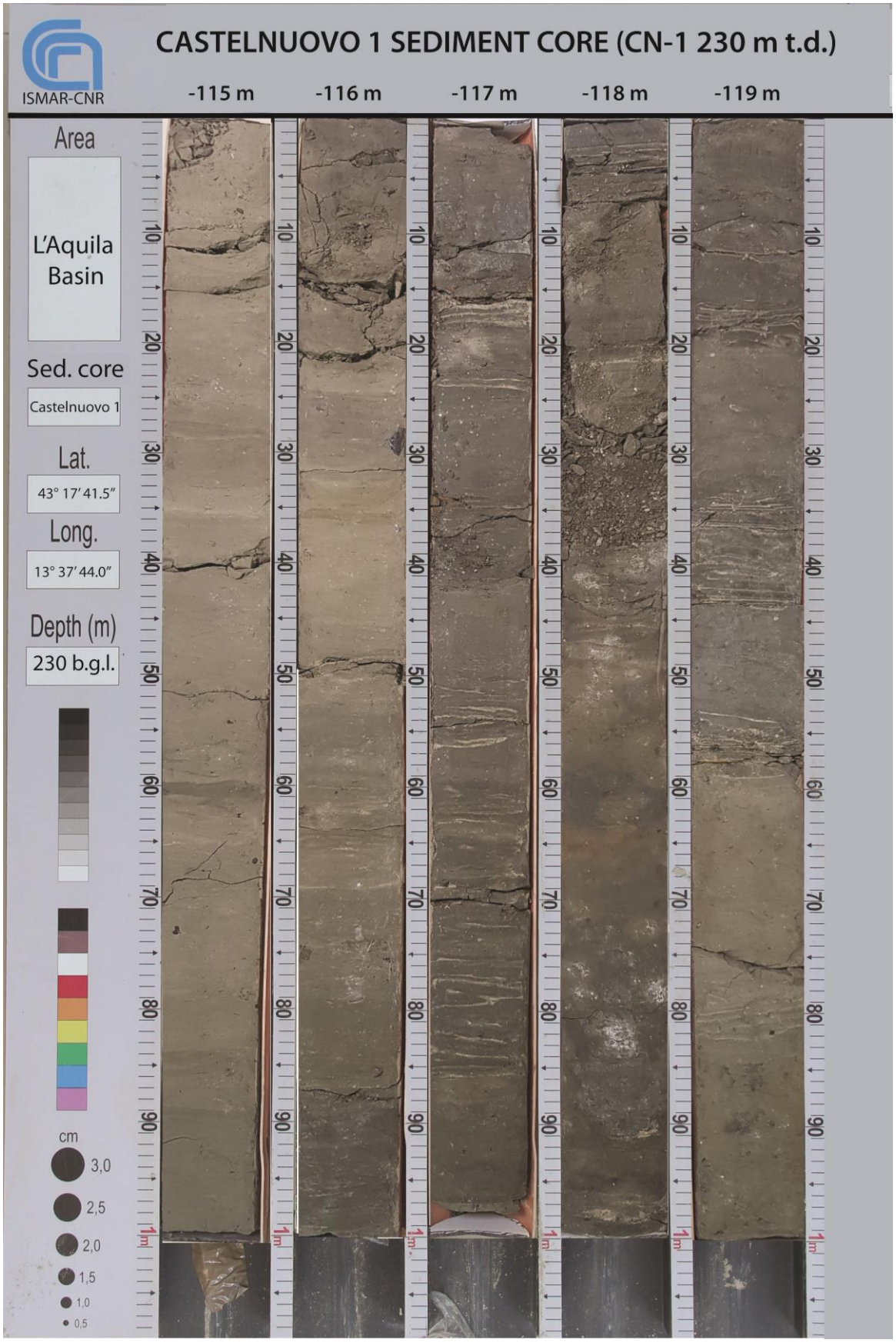

Fig. S1 – *CN-1 sediment core between -115 m to -120 m.*

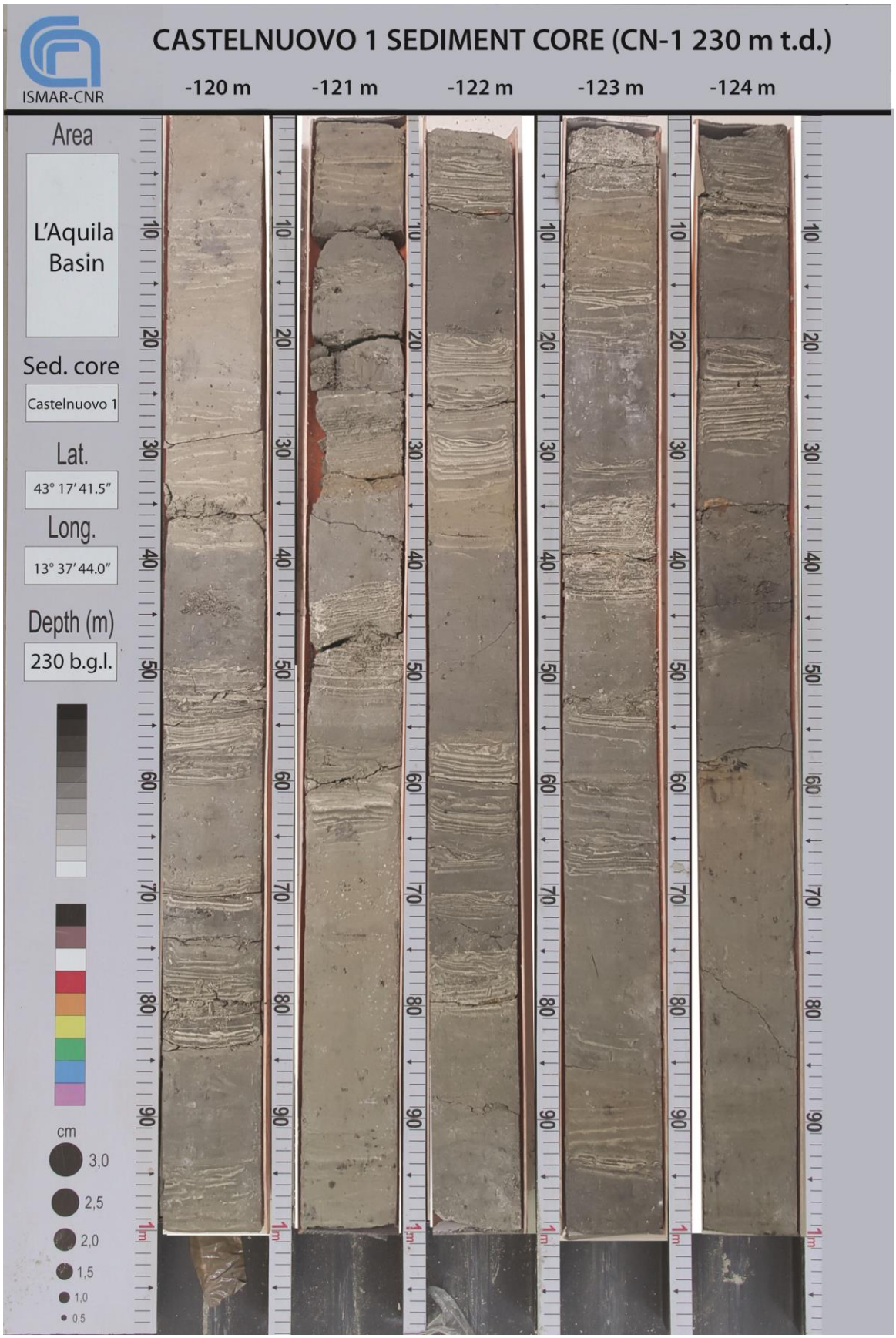

Fig. S2 – *CN-1 sediment core between -120 m to -125 m.*

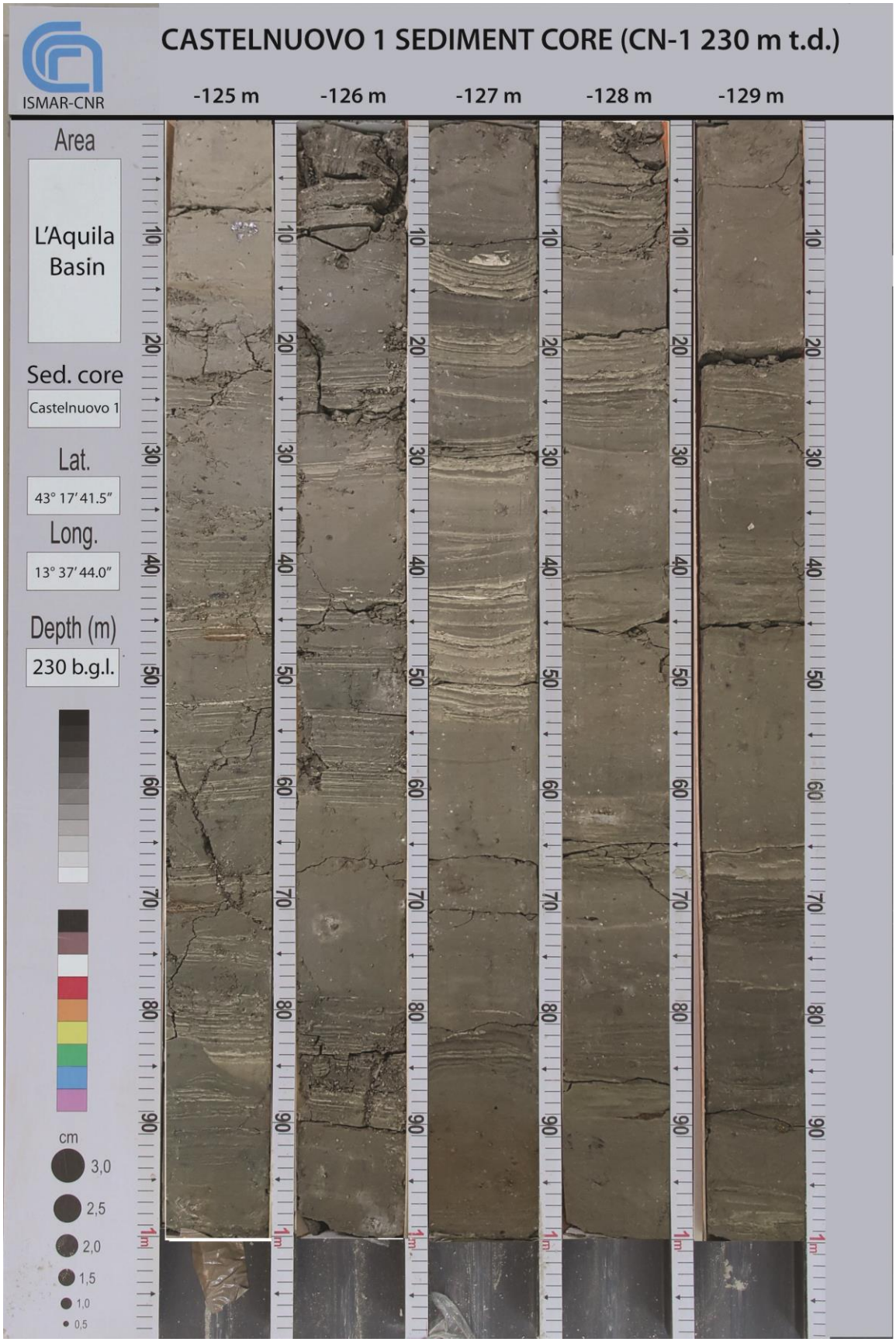

Fig. S3 – *CN-1 sediment core between -125 m to -130 m.*

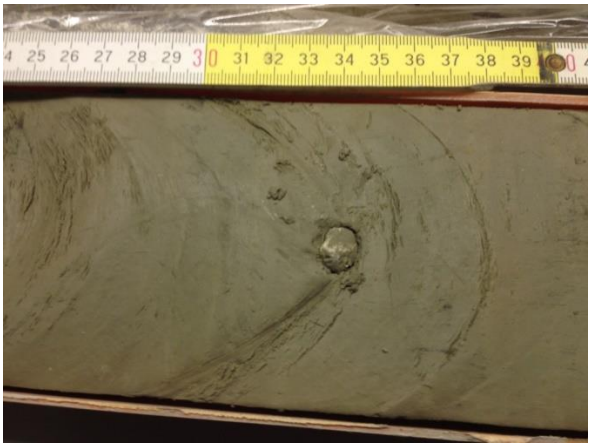

Fig. S4 – *CN-1 sediment core between -70.24 m to -70.40 m, showing the presence of a single outsized carbonate clast ("dropstone").*

Fig. S5 – *CN-1 sediment core between -126.00 m to -126.19 m, showing the presence of a single outsized carbonate clast ("dropstone").*

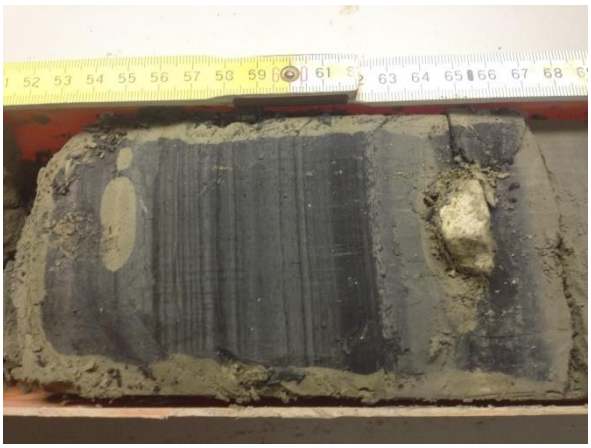

Fig. S6 – *CN-1 sediment core between -137.51 m to -137.69 m, showing the presence of a single outsized carbonate clast ("dropstone").*

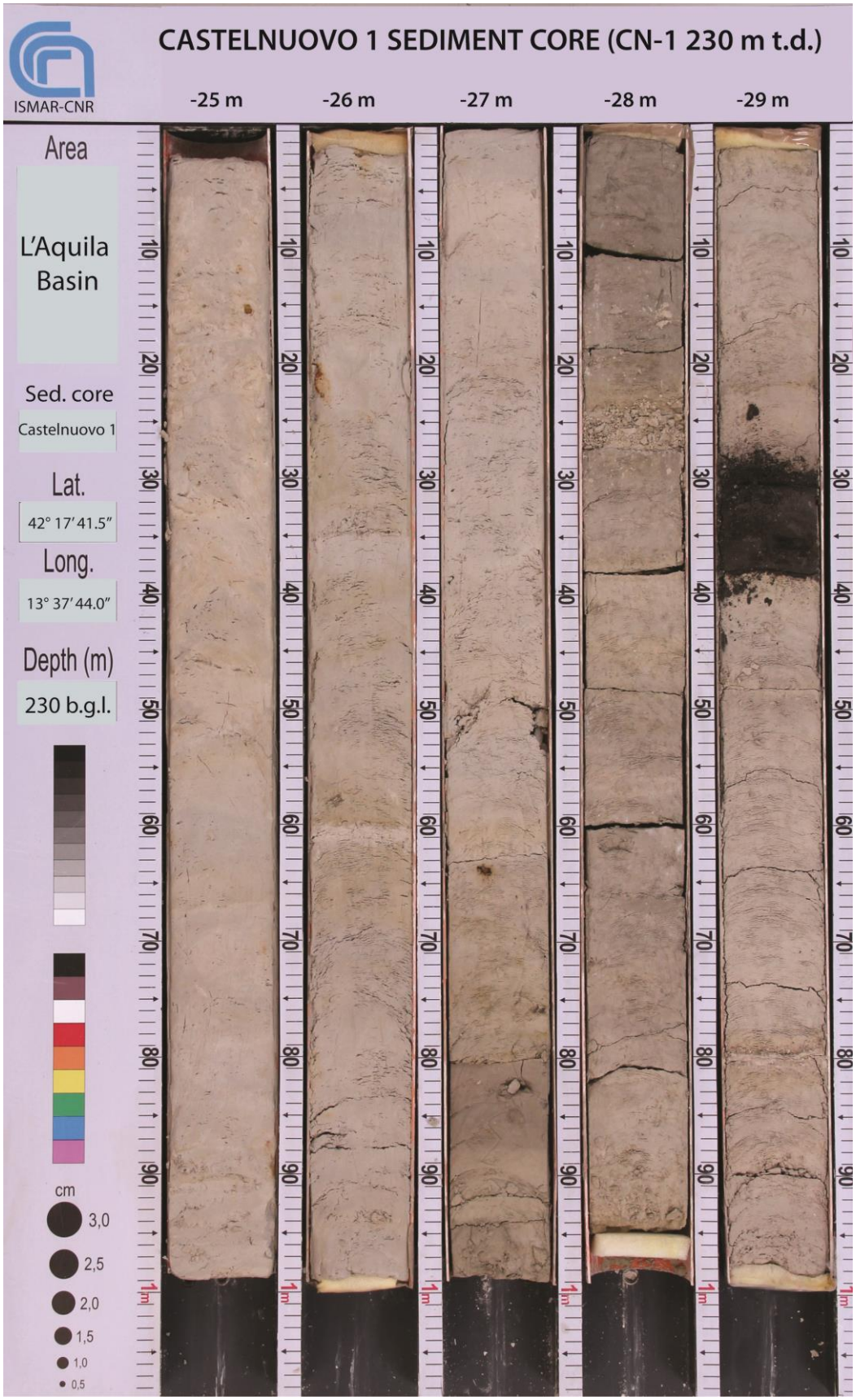

Fig. S7 – *CN-1 sediment core between -25.00 m to -30.00 m. The black layer between -29.28 m to -29.38 m is the tephra (CN 29.38) that corresponds to the tephra sampled from a cellar of Castelnuovo village (SNC-2), which has been $^{40}Ar/^{39}Ar$ dated to 1.77 ± 0.15 Ma.*

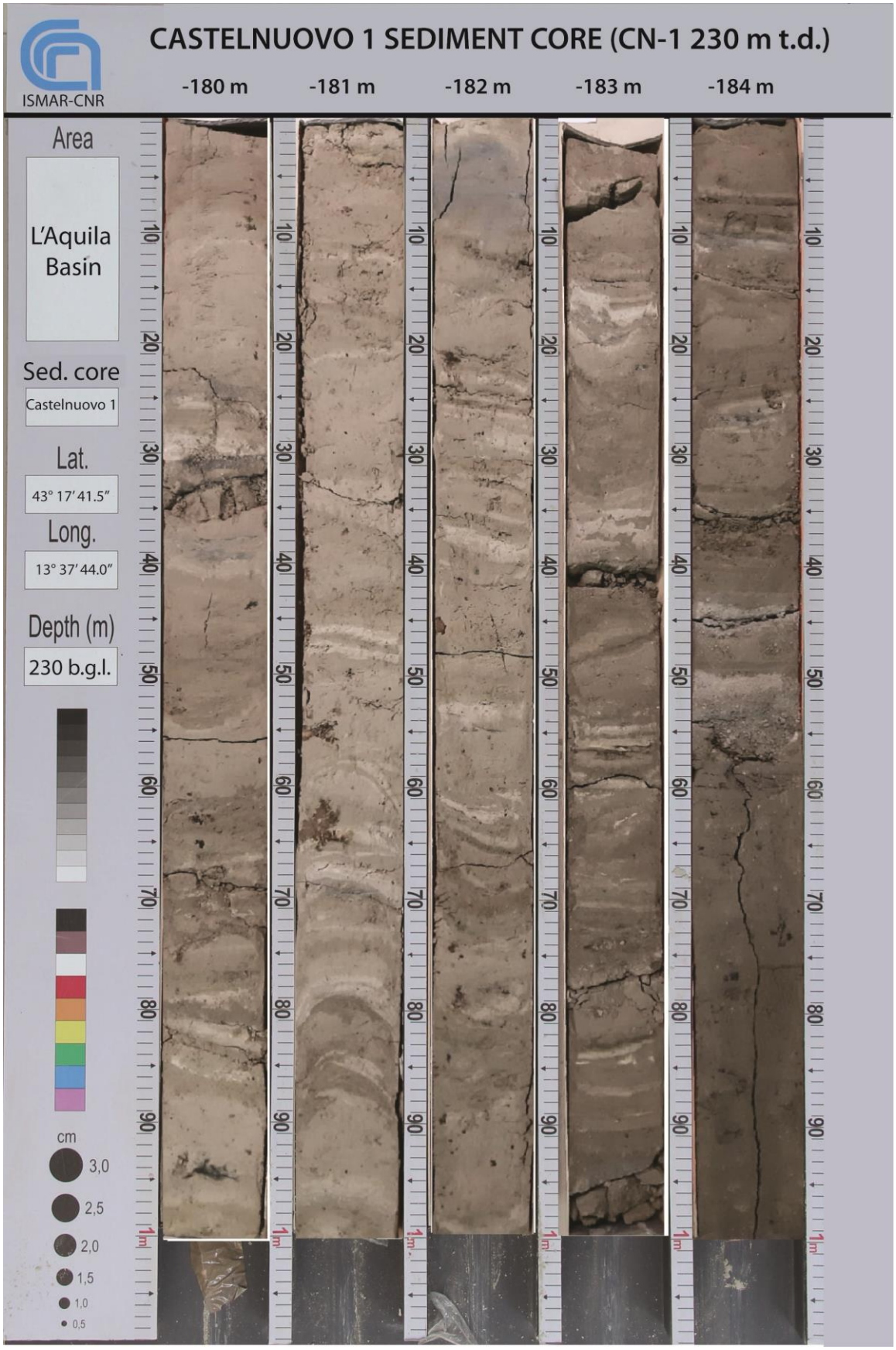

Fig. S8 – *CN-1 sediment core between -180.00 m to -185.00 m.*

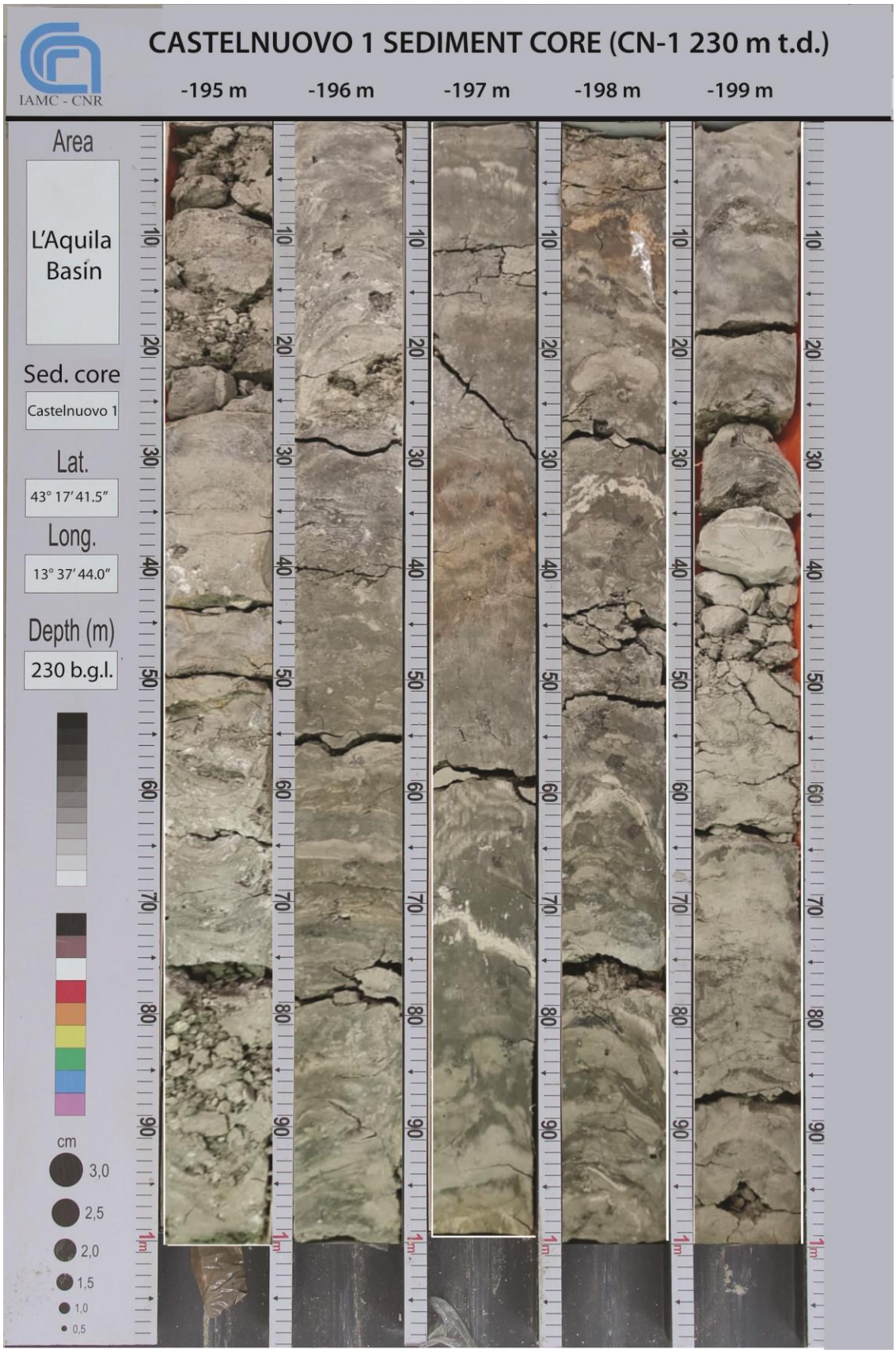

Fig. S9 – *CN-1 sediment core between -195.00 m to -200.00 m.*

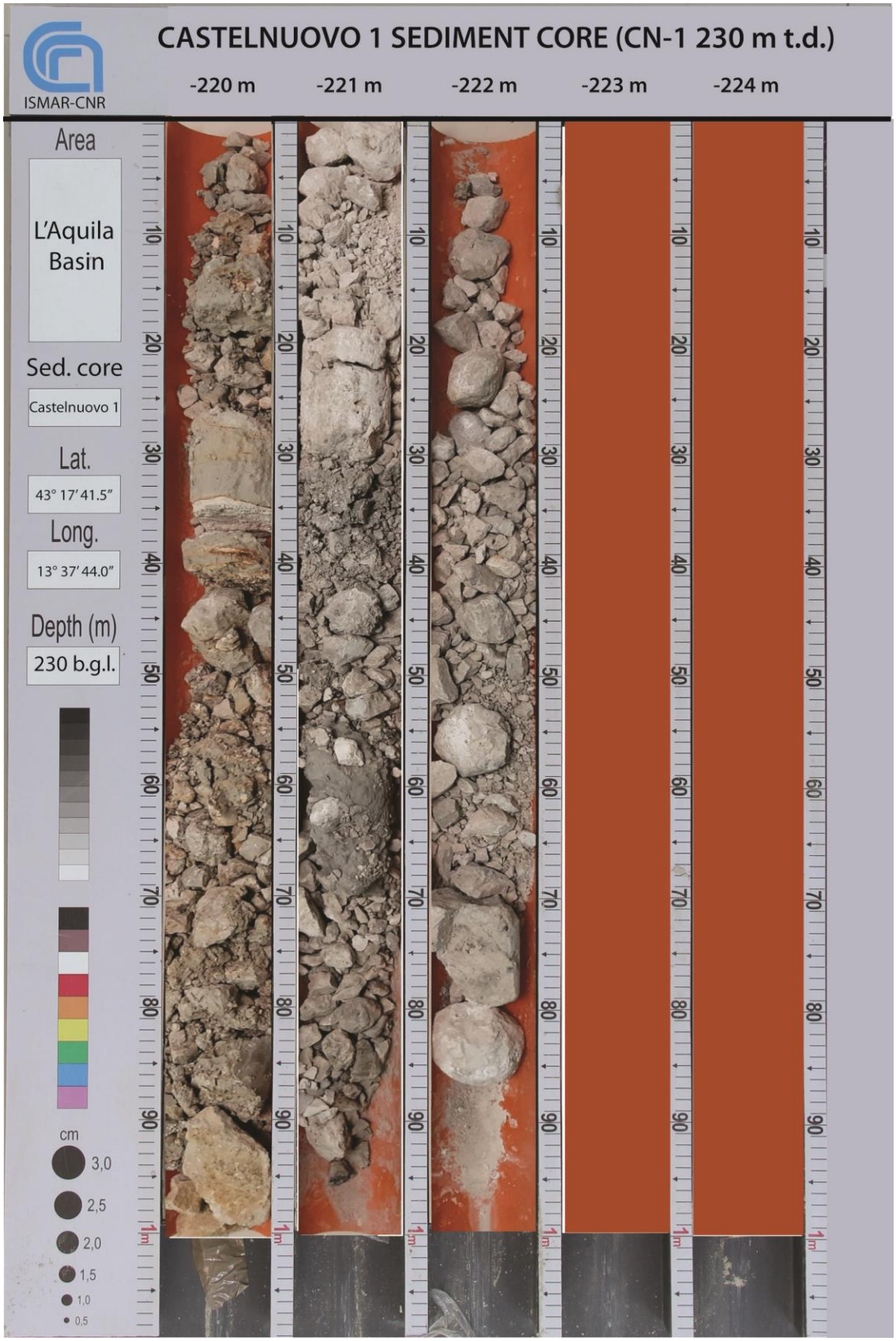

Fig. S10 – *CN-1 sediment core between -220.00 m to -223.00 m.*

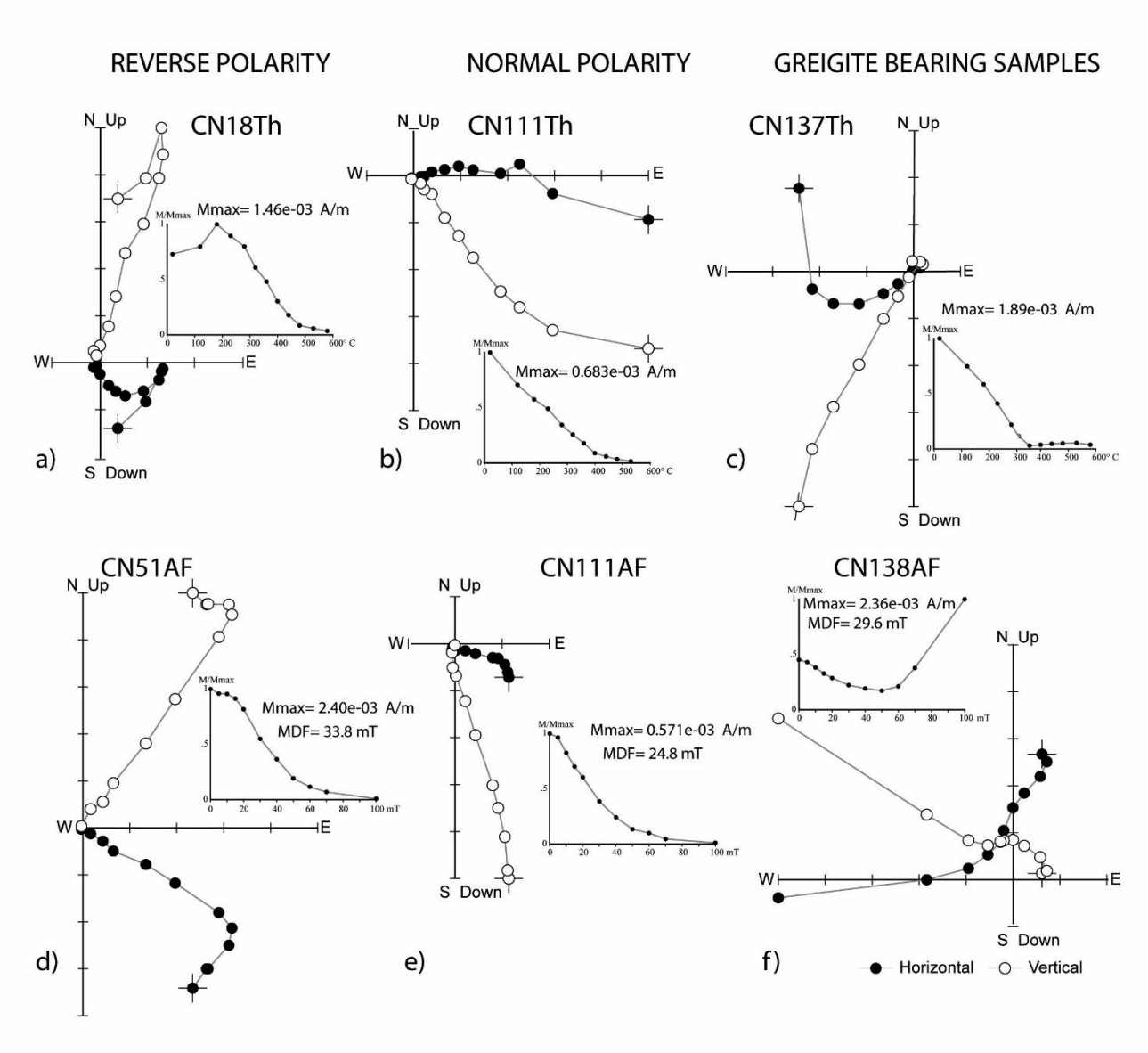

Figure S11 – *Representative demagnetization plots for selected specimens subjected to stepwise thermal demagnetization (a, b, c) and to stepwise AF demagnetization (d, e, f). The samples show demagnetization vectors aligned along linear paths towards the origin, after removal of a viscous low coercivity remanence component at the first demagnetization steps (5–10 mT for AF demagnetization; below 180-230°C for thermal demagnetization). For all the measured specimens a Characteristic Remanent Magnetization (ChRM) was determined by principal component analysis. The maximum angular deviation (MAD) for each determined ChRM direction was 4° on average, with a full range of variation between 0.5° and 21° for the specimens treated by AF demagnetization, and it was 6° on average, with a full range of variation between 0.6° and 31°, for the specimens treated by thermal demagnetization. Diagrams in a) and d) show typical behaviour for specimens with clear reverse polarity; specimens b) and e) show typical behaviour for specimens with clear normal polarity; diagrams in c) show typical behaviour for specimens with a maximum unblocking temperature (Tub) of 360 °C; diagrams in f) show typical behaviour for specimens which acquire a significant gyroremanent magnetization (GRM) at AF steps higher than 40-50 mT. The GRM acquisition is perpendicular to the axis of the magnetometer (i.e., perpendicular to the Z-axis of the specimens) and to the direction of the last AF demagnetization. Orthogonal vector diagrams: open and closed symbols represent projections onto vertical and horizontal planes, respectively.*

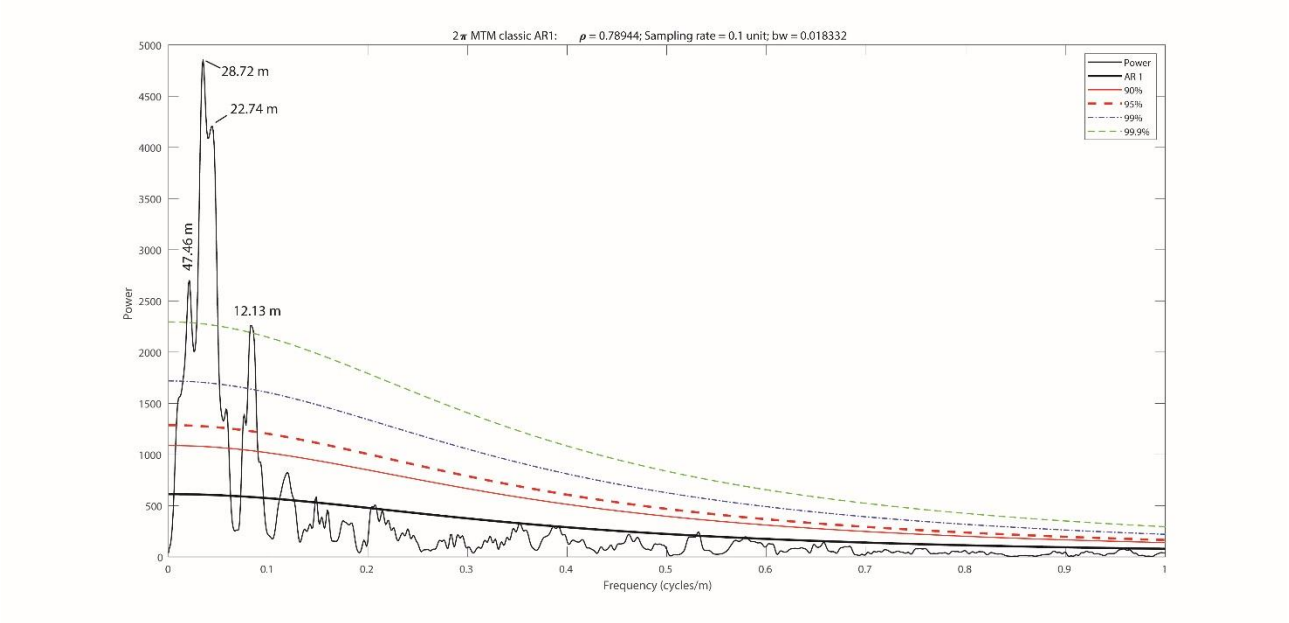

Figure S12 - *Periodogram showing main spectral density peaks highlighted by Multi-taper Method (MTM) spectral analysis, AR(1) modelling applied. Main frequency of 0.034814 cycles/m is related to a wavelength of 28.7240 m, with a secondary main peak marked by a frequency of 0.043976 cycles/m, referring to a wavelength of 22.7396 m.*

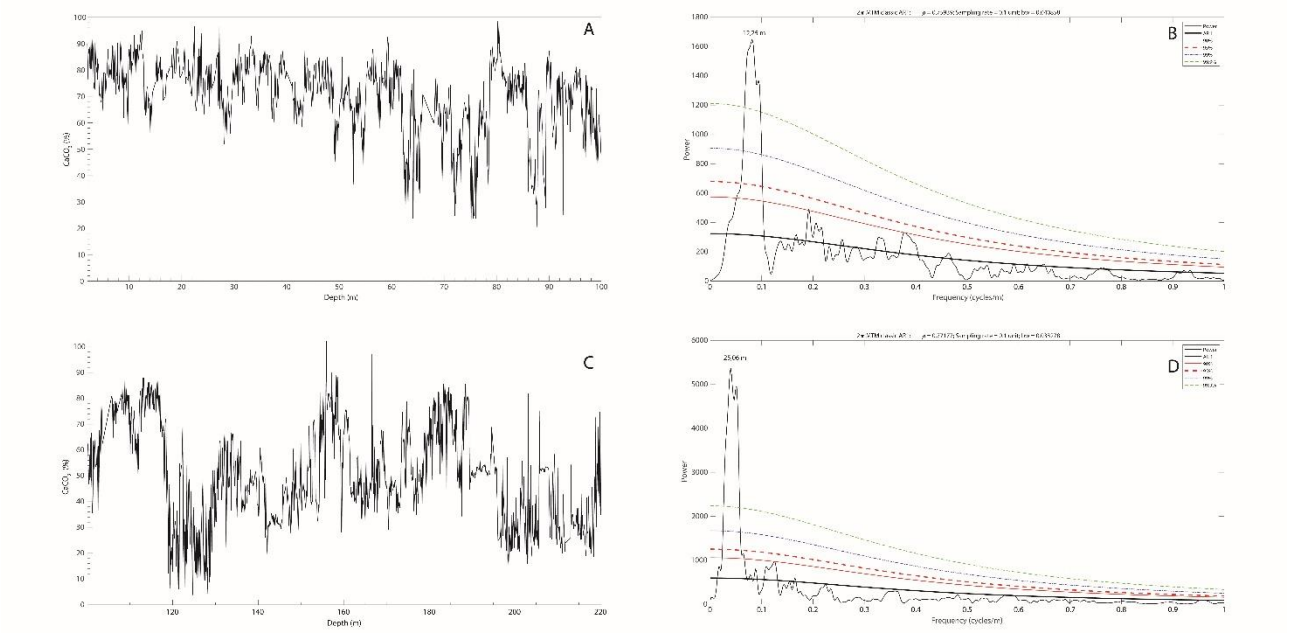

Figure S13 – *Splitting of the raw calcimetry data series. (**A**) First isolated sector of the calcimetry signal. (**B**) Periodogram of the first isolated sector of the calcimetry signal with the AR(1) modelling option. (**C**) Second isolated sector of the calcimetry signal. (**D**) Periodogram of the second isolated sector of the calcimetry signal with the AR(1) modelling option.*

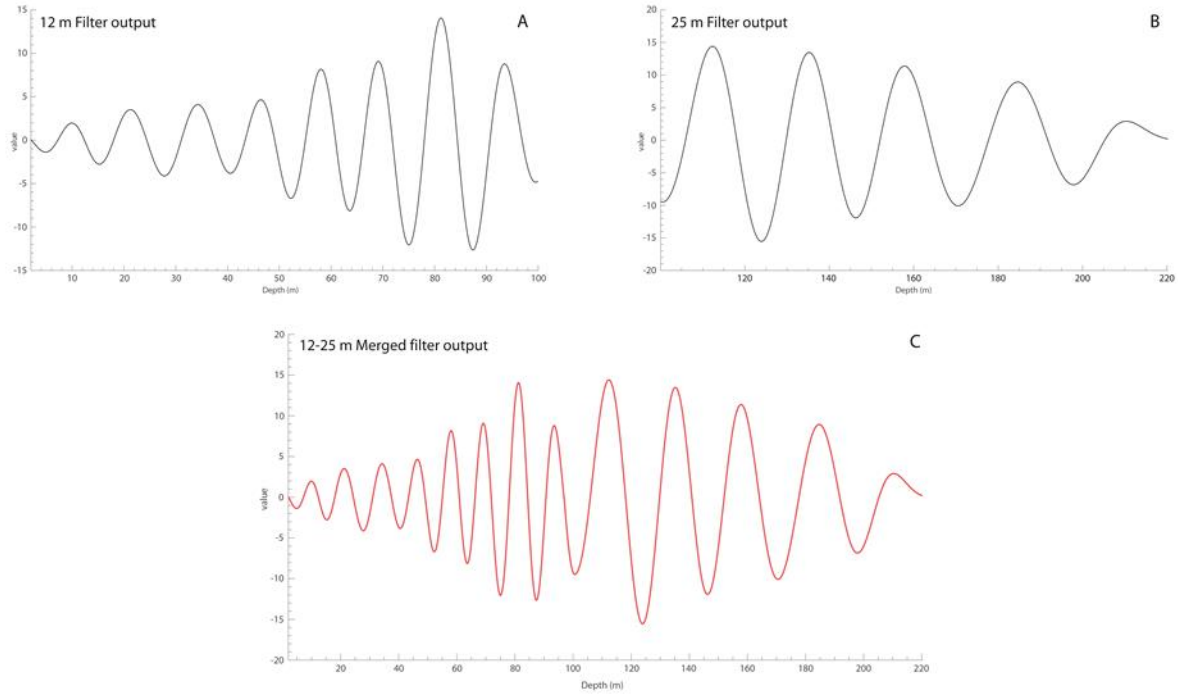

Figure S14 – *Filter output from the raw calcimetry data series after applying a Gaussian band-pass filter for filtering the main frequency. (**A**) 12 m filter output of the first isolated sector of the calcimetry signal. (**B**) 25 m filter output of the second isolated sector of the calcimetry signal. (**C**) Merged output filter of the whole calcimetry time series.*